Targeting the cMET pathway augments radiation response without adverse effect on hearing in NF2 schwannoma models

Yingchao Zhao[a,1,2], Pinan Liu[b,1], Na Zhang[a,1,3], Jie Chen[a,4], Lukas D. Landegger[c], Limeng Wu[a], Fu Zhao[b], Yanxia Zhao[a,2], Yanling Zhang[a], Jing Zhang[b], Takeshi Fujita[c], Anat Stemmer-Rachamimov[d], Gino B. Ferraro[a], Hao Liu[a], Alona Muzikansky[e], Scott R. Plotkin[f,g], Konstantina M. Stankovic[c], Rakesh K. Jain[a,5], and Lei Xu[a,5]

[a]Edwin L. Steele Laboratories, Department of Radiation Oncology, Massachusetts General Hospital and Harvard Medical School, Boston, MA 02114; [b]Department of Neurosurgery, Beijing Tian Tan Hospital, Capital Medical University, Beijing 100050, China; [c]Eaton Peabody Laboratories, Department of Otolaryngology, Massachusetts Eye and Ear and Harvard Medical School, Boston, MA 02114; [d]Molecular Pathology Division, Massachusetts General Hospital, Boston, MA 02114; [e]Division of Biostatistics, Massachusetts General Hospital and Harvard Medical School, Boston, MA 02114; [f]Department of Neurology, Massachusetts General Hospital, Boston, MA 02114; and [g]Cancer Center, Massachusetts General Hospital, Boston, MA 02114

Contributed by Rakesh K. Jain, December 29, 2017 (sent for review November 15, 2017; reviewed by Scott C. Floyd and Andrea Vambutas)

Neurofibromatosis type II (NF2) is a disease that needs new solutions. Vestibular schwannoma (VS) growth causes progressive hearing loss, and the standard treatment, including surgery and radiotherapy, can further damage the nerve. There is an urgent need to identify an adjunct therapy that, by enhancing the efficacy of radiation, can help lower the radiation dose and preserve hearing. The mechanisms underlying deafness in NF2 are still unclear. One of the major limitations in studying tumor-induced hearing loss is the lack of mouse models that allow hearing testing. Here, we developed a cerebellopontine angle (CPA) schwannoma model that faithfully recapitulates the tumor-induced hearing loss. Using this model, we discovered that cMET blockade by crizotinib (CRZ) enhanced schwannoma radiosensitivity by enhancing DNA damage, and CRZ treatment combined with low-dose radiation was as effective as high-dose radiation. CRZ treatment had no adverse effect on hearing; however, it did not affect tumor-induced hearing loss, presumably because cMET blockade did not change tumor hepatocyte growth factor (HGF) levels. This cMET gene knockdown study independently confirmed the role of the cMET pathway in mediating the effect of CRZ. Furthermore, we evaluated the translational potential of cMET blockade in human schwannomas. We found that human NF2-associated and sporadic VSs showed significantly elevated HGF expression and cMET activation compared with normal nerves, which correlated with tumor growth and cyst formation. Using organoid brain slice culture, cMET blockade inhibited the growth of patient-derived schwannomas. Our findings provide the rationale and necessary data for the clinical translation of combined cMET blockade with radiation therapy in patients with NF2.

schwannoma | cMET blockade | radiation | hearing test

Neurofibromatosis type 2 (NF2) is a dominantly inherited genetic condition with a birth prevalence of 1/25,000 (1). Bilateral vestibular schwannomas (VSs), which are nonmalignant tumors composed of neoplastic Schwann cells that arise from the eighth cranial nerve, are the hallmark of NF2 (2). VSs most commonly present with hearing loss and tinnitus, and can also cause dizziness, facial paralysis, other cranial neuropathies, and even death from brainstem compression. Standard treatments of VSs include surgical removal and radiation therapy (RT); however, both treatments can exacerbate hearing loss and cause deafness (3). Thus, the identification of a novel adjunct therapy that enhances VS radiosensitivity, and thereby lowers the radiation dose and the associated radiation-induced hearing loss, is urgently needed.

In patients with NF2 undergoing a clinical trial with bevacizumab, a humanized monoclonal antibody that specifically neutralizes VEGF-A, there was a reduction in the volume of most growing VSs and an improvement in hearing in 57% of patients (4). Despite this progress, a number of challenges remain: First, 43% of patients with NF2 did not respond to bevacizumab monotherapy, and, second, the hearing response was not durable (5). Recently, Blakeley et al. (6) reported that in patients with NF2-associated VS treated with bevacizumab, hearing improvements were inversely associated with baseline plasma hepatocyte growth factor (HGF) level, suggesting that

Significance

In patients with progressive vestibular schwannoma (VS), radiotherapy is associated with the risk of debilitating hearing loss. There is an urgent need to identify an adjunct therapy that, by enhancing the efficacy of radiation, can help lower the radiation dose and preserve hearing. In our newly developed cerebellopontine angle model of schwannomas that faithfully recapitulates the tumor-induced hearing loss, we demonstrate that cMET blockade sensitizes schwannomas to radiation therapy (RT) in neurofibromatosis type II schwannoma animal models without any adverse effects on hearing. Using an organoid brain slice culture model, cMET blockade inhibited the growth of patient-derived schwannomas. Our study provides the rationale and critical data for the clinical translation of combined cMET blockade with RT in patients with VSs.

Author contributions: L.D.L., S.R.P., K.M.S., R.K.J., and L.X. designed research; Y.c.Z., P.L., N.Z., J.C., L.D.L., L.W., F.Z., Y.x.Z., Y.l.Z., J.Z., T.F., A.S.-R., and H.L. performed research; Y.c.Z., P.L., N.Z., J.C., L.D.L., L.W., F.Z., Y.l.Z., J.Z., A.S.-R., G.B.F., H.L., A.M., K.M.S., and L.X. analyzed data; and P.L., L.D.L., F.Z., A.S.-R., A.M., S.R.P., K.M.S., R.K.J., and L.X. wrote the paper.

Reviewers: S.C.F., Duke University School of Medicine; and A.V., Hofstra/Northwell School of Medicine, Feinstein Institute for Medical Research.

Conflict of interest statement: R.K.J. received consultant fees from Merck, Ophthotech, Pfizer, Sun Pharma Advanced Research Corporation, SynDevRx, and XTuit; owns equity in Enlight, Ophthotech, SynDevRx, and XTuit; and serves on the Board of Directors of XTuit and the Boards of Trustees of Tekla Healthcare Investors, Tekla Life Sciences Investors, Tekla Healthcare Opportunities Fund, and Tekla World Healthcare Fund. No funding or reagents from these companies were used in these studies.

[1]Y.c.Z., P.L., and N.Z. contributed equally to this work.

[2]Present address: Cancer Center, Union Hospital, Tongji Medical College, Huazhong University of Science and Technology, Wuhan, 430023 Hubei, China.

[3]Present address: Department of Otolaryngology Head and Neck Surgery, Beijing TongRen Hospital, Capital Medical University, 100730 Beijing, China.

[4]Present address: Department of Oral and Maxillofacial Surgery, Xiangya Hospital, Central South University, Changsha, 410008 Hunan, China.

[5]To whom correspondence may be addressed. Email: jain@steele.mgh.harvard.edu or lei@steele.mgh.harvard.edu.

This article contains supporting information online at www.pnas.org/lookup/suppl/doi:10.1073/pnas.1719966115/-/DCSupplemental.

Published online February 9, 2018.

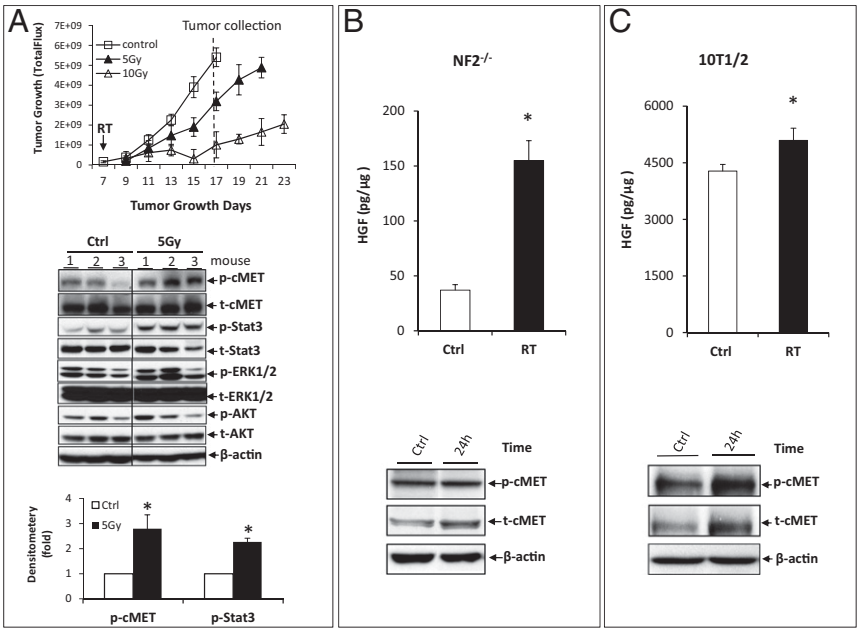

Fig. 1. RT activates cMET signaling in NF2$^{-/-}$ schwannoma xenografts. (*A*) In the NF2$^{-/-}$ sciatic nerve model, when tumors reached 2.5 mm in diameter, mice were randomized into control (Ctrl) or radiation groups (5 Gy and 10 Gy). Mice were killed when tumors in the Ctrl group reached 1 cm in diameter. Protein samples were extracted, and various signaling pathways were analyzed by Western blot analysis and quantified by densitometry using ImageJ ($n = 3$ for each group). p-, phosphorylation. The effect of radiation (8 Gy) on HGF expression (analyzed by ELISA, all assays were performed in triplicate) and on p-cMET (analyzed by Western blot, repeated three times) was studied in NF2$^{-/-}$ cells (*B*) and a fibroblast 10T1/2 cell line (*C*). *$P < 0.01$ (Student *t* test).

HGF/cMET signaling may play a role in hearing loss and affect the response of schwannoma to bevacizumab treatment.

HGF, first identified in the serum of hepatectomized rats as a potent mitogen for primary hepatocytes, is now known to be a key player in the malignant cross-talk between the tumor and stroma (7–9). In malignant tumors, HGF is produced by a variety of stromal mesenchymal cells, and its protooncogene receptor, cMET, is expressed by cancer cells. In a number of major human cancers, both HGF expression and cMET expression have been shown to be deregulated and to correlate with a poor prognosis (10–12). Upon HGF binding, cMET activates downstream signaling pathways and induces pleiotropic biological activities, including cell proliferation, cell–cell dissociation, migration, and angiogenesis (13–15). More importantly, increasing evidence implicates cMET as a major mechanism of resistance to chemotherapy, RT, and targeted therapies (16–18). In human sporadic VSs, the expression of cMET has been detected (19, 20), and it has been found to be elevated in comparison to normal nerve tissues (21). However, whether cMET and HGF expression and activation correlate with schwannoma progression is not known. Studies of the functional role of HGF/cMET in schwannoma progression are also limited. In particular, HGF has been shown to be a mitogen for Schwann cells in vitro (22). A recent study showed that cMET blockade inhibits schwannoma growth in an animal model (23). This information, together with the inverse correlation between HGF- and bevacizumab-induced hearing response, prompted us to investigate whether HGF/cMET blockade can enhance radiation efficacy and help lower radiation dose. Using our cerebellopontine angle (CPA) model for schwannomas, we

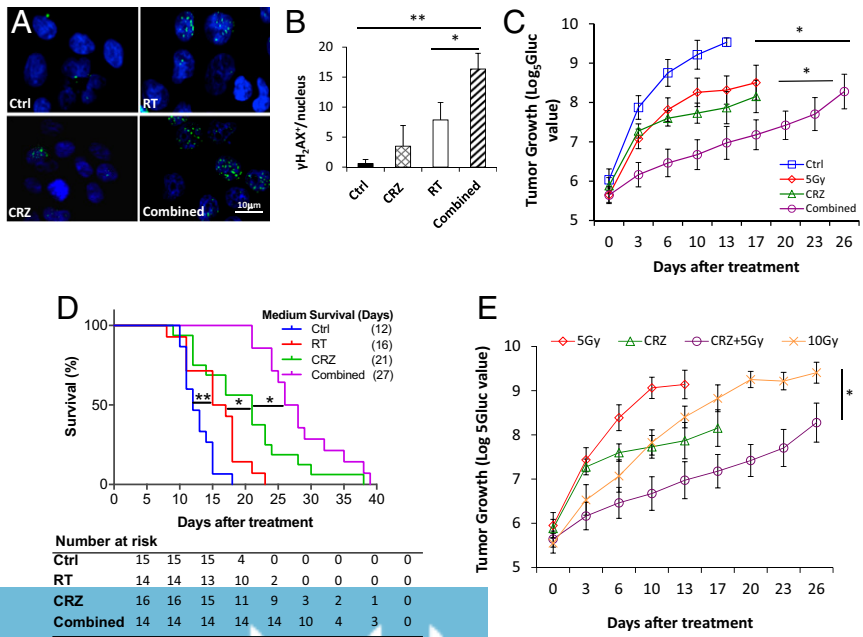

Fig. 2. Combined cMET blockade and RT shows improved efficacy in schwannoma models. (*A*) Representative images of immunofluorescent staining of gamma histone H2AX (γH_2AX) in NF2$^{-/-}$ schwannoma cells treated with control (Ctrl), CRZ (2 μM), RT (8 Gy), or combined CRZ and RT (Combined) for 24 h. (*B*) Quantification of the number of γH_2AX^+ foci/nuclei was done using ImageJ software. All assays were performed in triplicate. *$P < 0.05$; **$P < 0.01$ (Student *t* test). (*C*) Growth curve of Gluc-transduced NF2$^{-/-}$ tumor in the sciatic nerve model. Growth of nontreated (Ctrl), CRZ (50 mg/kg), 5 Gy irradiated (RT), and Combined tumors was measured by plasma Gluc level tested by a luminometer every 3 d. *$P < 0.01$. (*D*) Survival curve of mice bearing NF2$^{-/-}$ tumors in CPA models ($n = 15$, $n = 14$, $n = 16$, and $n = 14$ in Ctrl, RT, CRZ, and Combined groups, respectively). Representative of at least three independent experiments, data are presented as mean ± SEM. *$P < 0.01$; **$P < 0.005$. (*E*) Growth of NF2$^{-/-}$ tumors in mice treated with Ctrl, CRZ, 5 Gy of RT, 10 Gy of RT, or CRZ combined with 5 Gy of RT as measured by Gluc level ($n = 10$). Representative of at least three independent experiments, all data are presented as mean ± SEM. *$P < 0.05$.

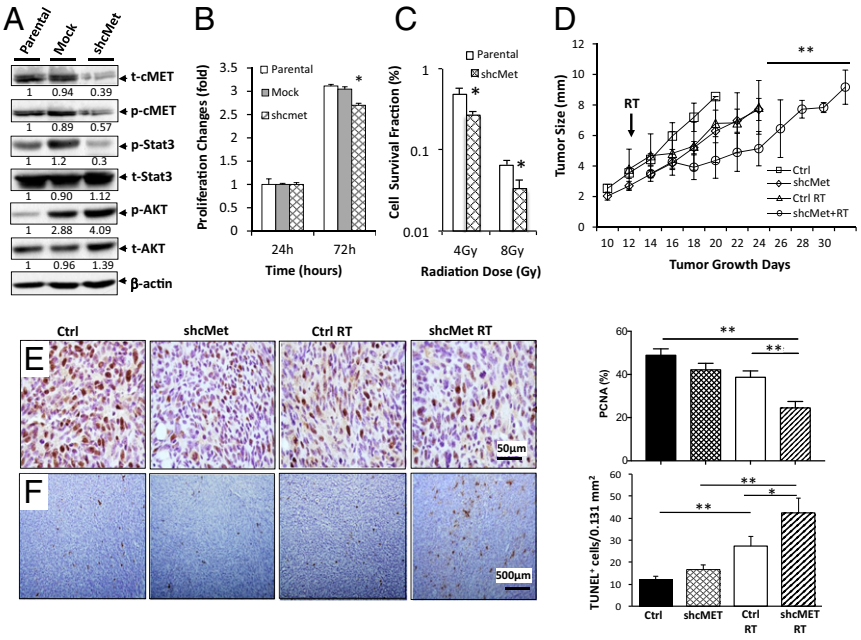

Fig. 3. MET gene knockdown decreases schwannoma growth and increases radiation sensitivity. (*A*) Effects of stable transfection of cMET shRNA on cMET expression and its downstream signaling pathway activation as evaluated by Western blot analysis. p-, phosphorylation; shcMet, short hairpin cMET; t-, total expression. The effects of cMET knockdown on schwannoma cell proliferation as evaluated by MTT assay (*B*) and on radiosensitivity as evaluated by colony formation assay (*C*) are shown. All assays were performed in triplicate. $*P < 0.05$ (Student *t* test). (*D*) Growth curve for $NF2^{-/-}$ schwannomas in the sciatic nerve model. Growth of mock-transfected (Ctrl), shcMet-transfected, 5 Gy irradiated mock control (Ctrl RT), and shcMet+RT tumors was measured by caliper every 3 d ($n = 8$). Representative of at least three independent experiments, all data are presented as mean ± SEM. $**P < 0.01$. Representative IHC-stained tissue sections and quantification of proliferating cell nuclear antigen (PCNA) for proliferating cells (*E*) and TUNEL for apoptotic cells (*F*) are shown ($n = 4$ mice per group, 10 random fields were chosen for quantification). $*P < 0.05$; $**P < 0.01$ (Student *t* test).

demonstrate that cMET blockade is effective against both mouse and human schwannomas.

Results

cMET Signaling Is Activated in Schwannomas Resistant to Radiation. In the mouse $NF2^{-/-}$ sciatic nerve model, tumors initially continued to grow for several days postradiation before shrinking. However, tumor shrinkage was transient, with subsequent progression seen in all cases (Fig. 1*A*). To determine the mechanisms of radiation resistance, we evaluated the activation status of several signaling pathways. We found that in both $NF2^{-/-}$ (Fig. 1*A*) and HEI-193 (Fig. S1*A*) schwannoma cells, radiation significantly activated cMET and its downstream Stat3 pathway but did not change the phosphorylation or total expression of ERK1/2 and Akt MAPK.

In non-VS tumors, HGF is synthesized and secreted by stromal cells, such as fibroblasts, and cMET is activated in the tumor cells (7, 8). Hence, we irradiated $NF2^{-/-}$ (Fig. 1*B*) and HEI-193 (Fig. S1*B*) schwannoma cell lines and a myofibroblast cell line (10T1/2; Fig. 1*C*) with 8 Gy of radiation in vitro, and found that radiation significantly induced HGF expression and cMET phosphorylation in both tumor and stromal cells.

cMET Blockade Enhances Radiosensitivity by Enhancing DNA Damage. We used crizotinib (CRZ) to block cMET signaling in schwannomas. CRZ is a protein kinase inhibitor of cMET, ALK, and ROS1, and it is approved by the US Food and Drug Administration to treat locally advanced or metastatic non-small cell lung cancers. CRZ treatment significantly reduced cMET phosphorylation and its downstream Stat3 activation (Fig. S1*C*), and significantly inhibited the proliferation of $NF2^{-/-}$ and HEI-193 (Fig. S1*D*) schwannoma cells in vitro. To evaluate synergy, we used Chalice Bioinformatics Software to calculate the Loewe excess. A synergy score of 2.96 indicates synergistic effects between CRZ and RT. To evaluate DNA damage signaling, we evaluated the number of phosphorylated γ-H2AX foci. Thirty minutes after irradiation, the number of γ-H2AX phosphorylation$^+$ foci was too high to distinguish individual foci, and differences were not distinguishable between RT alone or combined RT+CRZ. At 24 h after irradiation, in the RT alone group, the amount of γ-H2AX phosphorylation$^+$ foci/nuclei decreased to 7.86 ± 2.8, while in the combined RT+CRZ group, it remained at a significantly higher level: 16.35 ± 3.2 (Fig. 2 *A* and *B*). This persistence of γ-H2AX phosphorylation indicates that CRZ impaired DNA repair, rendering the tumor cells more sensitive to irradiation.

Combined cMET Blockade and RT Shows Improved Efficacy in Schwannoma Models. In the $NF2^{-/-}$ sciatic nerve (Fig. 2*C*) and CPA model (with murine $NF2^{-/-}$ cells allografted into the CPA; Fig. 2*D*), combined CRZ and radiation treatments significantly inhibited tumor growth and extended survival over CRZ or RT monotherapy. The same effect of CRZ-enhanced radiation efficacy was also observed in the HEI-193 schwannoma model (Fig. S1*E*). Immunohistochemical (IHC) staining confirmed that CRZ treatment decreased the percentage of proliferating tumor cells. More importantly, it significantly increased the number of apoptotic tumor cells compared with radiation monotherapy (Fig. S2 *A* and *B*). RT treatment damaged blood vessels, reducing microvessel density and vessel perfusion; as a result, tumors became more hypoxic. CRZ treatment had no effect on vessel density or on perfusion; therefore, tumor oxygenation did not change (Fig. S2 *C* and *D*).

To determine if combining cMET blockade with RT would lower the radiation dose needed to control schwannoma growth, and would thus minimize RT adverse effects, we treated groups of mice with (*i*) CRZ, (*ii*) 5 Gy of radiation, (*iii*) 10 Gy of radiation, or (*iv*) CRZ + 5 Gy of radiation and compared our results with those of no-treatment controls. We found 10 Gy of radiation to be significantly more effective than 5 Gy. However, when combined with CRZ treatment, 5 Gy of radiation was more effective than 10 Gy of radiation alone (Fig. 2*E*).

cMET Gene Knockdown Suppresses Schwannoma Tumor Growth and Enhances Radiation Sensitivity. As CRZ blocks several kinases, we knocked down cMET expression in schwannoma cell lines using lentiviral short hairpin RNA against cMET (cMET-shRNA) to confirm that the effect of CRZ is mediated via blocking cMET signaling. A random sequence with no homology to any mouse genes was used as a transfection control (mock). Infection of cMET-shRNA decreased cMET expression and its downstream Stat3 activation (Fig. 3*A*). In vitro, cMET knockdown inhibited tumor cell growth (Fig. 3*B*), and increased tumor cell radiosensitivity (Fig. 3*C*). After implantation in the sciatic nerve, cMET knocked-down cells (cMET-shRNA) produced slower growing

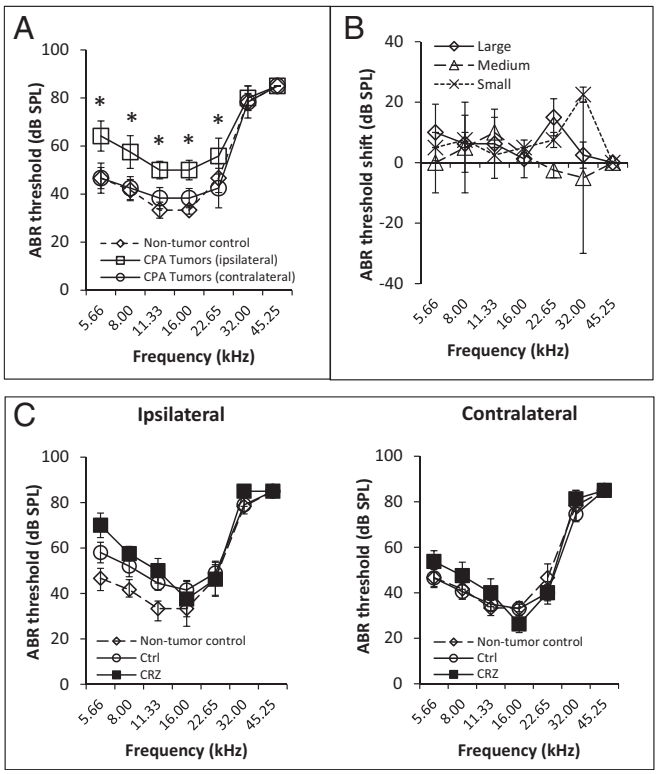

Fig. 4. cMET blockade does not improve hearing. (*A*) Mice with $NF2^{-/-}$ schwannomas in the CPA model ($n = 6$) have elevated ABR thresholds ipsilateral to the tumor compared with thresholds contralateral to the tumor or thresholds in nontumor-bearing control mice ($n = 3$). The significance of results is depicted by asterisks. (*B*) In the $NF2^{-/-}$ schwannoma CPA model, measurement of ABR threshold shifts [ipsilateral minus contralateral to the tumor; $n = 8$ mice; two mice with a small tumor (Gluc $< 1.0 \times 10^5$ units, 10 mm^3), two mice with a medium-sized tumor (Gluc 1.0×10^5–3.0×10^6 units, 10–40 mm^3), and four mice with a large tumor (Gluc $> 3.0 \times 10^6$ units, >40 mm^3)]. (*C*) Measurements of ABR thresholds in nontumor-bearing mice ($n = 3$) and in $NF2^{-/-}$ tumor-bearing mice of control (Ctrl; $n = 10$) and CRZ-treated ($n = 7$) groups (ipsilateral and contralateral to the CPA schwannomas). Data are presented as mean ± SEM.

tumors that were more sensitive to RT compared with mock control tumors (Fig. 3*D*). IHC staining confirmed that RT had a greater effect in inhibiting tumor cell proliferation and increasing tumor cell apoptosis in cMET knocked-down tumors compared with mock control tumors (Fig. 3 *E* and *F*).

cMET Blockade Has No Adverse Effect on Hearing. Using our newly developed CPA model, we implanted schwannoma cells in the CPA area close to the root entry zone of the eighth cranial nerve (Fig. S3 *A* and *B*). To ensure that the surgical technique involving skull drilling for a craniotomy and needle injections for tumor cell implantation did not cause hearing loss, we measured distortion product otoacoustic emissions (DPOAEs; reflecting outer hair cell function) and auditory brainstem responses (ABRs; reflecting activity of the auditory nerve and brainstem nuclei) ipsilateral and contralateral to saline injections vs. those in uninjected control mice (Fig. S3*C*). We did not detect statistically significant differences between the groups; the lowest corrected *P* value for any frequency-specific Kruskal–Wallis test was 0.26. This indicates that any hearing loss observed in subsequent experiments is unrelated to the surgical technique or injection itself.

To assess the effect of tumor growth on hearing function, we compared DPOAE and ABR thresholds ipsilateral and contralateral to tumor cell implantation vs. those in nontumor-bearing control mice. ABR thresholds contralateral to the tumor cell injection were not significantly different from those in nontumor-bearing mice, whereas ABR thresholds ipsilateral to the tumor cell injection were higher than on the contralateral side, suggesting that hearing loss was due to the CPA tumor ($P = 0.03$ for 5.6, 8.0, and 22.6 kHz and $P = 0.01$ for 11.3 and 16.0 kHz) (Fig. 4*A*). DPOAE thresholds demonstrated a trend in some frequencies, but did not reach statistical significance ($P = 0.05$ for 11.3 and 16.0 kHz) (Fig. S4*A*).

To assess whether tumor size affects the magnitude of tumor-induced shifts in auditory thresholds, we measured auditory thresholds in mice bearing small (<10 mm^3), medium (10–40 mm^3), and large (>40 mm^3) tumors (Fig. S3*D*). We did not detect statistically significant differences in ABR (Fig. 4*B*) or DPOAE (Fig. S4*B*) threshold shifts between the mice bearing small, medium, and large tumors. Detailed responses from individual animals are shown in Fig. S4*C*. When analyzing the Spearman correlation between the Gaussia luciferase (Gluc) value (reflecting the size of a Gluc-transduced tumor; Fig. S3*D*) and the average DPOAE or ABR thresholds across all frequencies for all eight mice, the Spearman correlation coefficient was low (0.50 and 0.16, respectively). These results in mice are consistent with the observation in human patients whose VS size does not correlate with the severity of hearing loss (24).

In nontumor-bearing normal mice (Fig. S4*D*), as well as in mice bearing CPA tumors (Fig. S4*E*), we did not observe DPOAE and ABR thresholds change 3 wk after RT (5 Gy). When evaluating the effect of CRZ on hearing, no changes in ABR thresholds were observed after CRZ treatment (Fig. 4*C*). There was a nonsignificant trend for elevated DPOAE thresholds in the CRZ-treated animals compared with untreated control animals. This trend was particularly pronounced in DPOAE thresholds when comparing the ipsilateral and contralateral DPOAE averages at 16.00 and 22.65 kHz for each group ($P = 0.10$) (Fig. S4*F*). Several studies of inner ear disease have reported that HGF protects hair cells and improves hearing (25–27). However, HGF levels appear to be tightly regulated, as too much or too little HGF is associated with hearing loss (28). In our schwannoma model, we found that $NF2^{-/-}$ tumor implanted in the CPA model demonstrated significantly elevated HGF production compared with normal nontumor brain, and CRZ treatment did not change HGF production (Fig. S4*G*).

Expression of HGF and Activation of cMET Correlate with Tumor Growth in Human Schwannoma Specimens. To explore the translational potential of blocking HGF/cMET signaling in patients with NF2, we first validated target expression by profiling the HGF/cMET pathways using microarray (Fig. 5*A*). We included 17 NF2-associated VSs and 10 sporadic VSs, and compared them with four normal great auricular nerves. The baseline characteristics of the patients in the study are shown in Table 1. The median relative cMET mRNA levels were significantly higher in both NF2 VSs (10.07 ± 1.43) and sporadic VSs (11.73 ± 1.05) compared with normal nerves (9.51 ± 0.44; $P = 0.019$). The median relative HGF mRNA level was not significantly different in NF2-associated VSs (7.29 ± 0.97) or sporadic VSs (7.17 ± 0.9) compared with normal nerves (7.70 ± 0.74; $P = 0.638$) (Fig. 5*B*). HGF binding to cMET induces autophosphorylation of two MET tyrosine residues, Y1234 and Y1235, which results in the binding and phosphorylation of adaptor proteins, such as Gab-1, Grb2, Shc, and c-Cbl, and subsequent activation of signal transducers, such as PI3K, PLC-γ, STATs, ERK1/2, and FAK (29). We found elevated expression of HGF/cMET adaptor and effector molecules in NF2-associated and sporadic VSs compared with normal nerves (Fig. 5*C*).

The RNA data were validated at the protein level by IHC staining of HGF and phosphorylated cMET in an independent

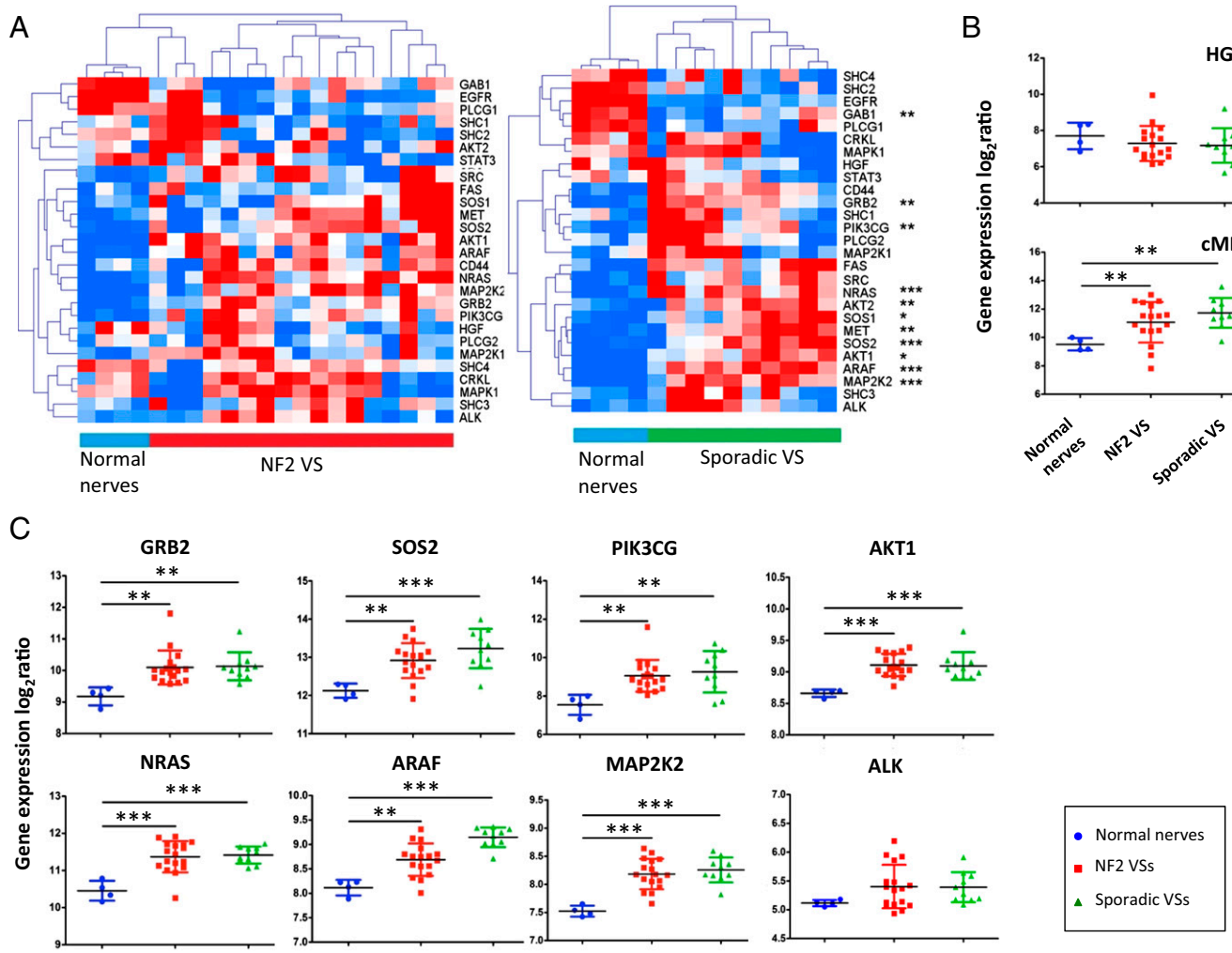

Fig. 5. cMET signaling pathway is activated in human schwannomas. (*A*) Microarray expression heat map of the HGF/cMET pathway genes in NF2-associated VSs ($n = 17$) and in sporadic VSs ($n = 10$) compared with normal great auricular nerves ($n = 4$). Red indicates increased expression relative to the overall set of samples, and blue indicates decreased expression relative to the overall set of samples. The expression levels of HGF and cMET (*B*) and their adaptor and effector molecules (C) in normal nerves, NF2-associated VSs, and sporadic VSs are shown. RMA log2-normalized expression values are shown. $*P < 0.05$; $**P < 0.005$; $***P < 0.0005$.

cohort of 29 paraffin-embedded NF2-associated VS samples (Table 2). We found HGF protein expression in the tumor cell cytoplasm and the tumor extracellular matrix. Pathological scoring (Fig. S5) revealed that VSs with a cyst (>1 cm) had a higher HGF staining intensity than tumors without a cyst ($P = 0.005$, χ^2 test). Phosphorylated cMET was detected in 15 of 29 VSs (51.7%), and its expression level positively correlated with tumor volume ($\gamma = 0.378$, $P = 0.043$).

cMET Blockade Inhibits the Growth of Patient-Derived Schwannomas in Organotypic Brain Slice Culture. To further examine the clinical translational potential of cMET blockade in patients with schwannomas, we used an organotypic cerebellar brain slice culture model. This model allowed us to test the effect of CRZ on patient-derived schwannomas grown in the brain microenvironment. To validate the model, brain slices implanted with GLuc-transduced $NF2^{-/-}$ cells were treated with CRZ and compared with untreated controls. CRZ treatment significantly inhibited tumor cell growth over time (Fig. S6 *A* and *B*). After validating the model with labeled cells, we cultured chunks of human NF2-associated VSs and meningiomas (obtained from indicated surgeries) in the brain slice cultures. CRZ treatment significantly decreased cMET phosphorylation and tumor cell proliferation, and increased tumor cell apoptosis (Fig. 6).

Discussion

Over the past few decades, RT has become a standard treatment for VS. However, two major issues limit the efficacy of RT in VS: (*i*) radiation toxicity that leads to debilitating hearing loss, often causing social isolation and depression, and (*ii*) the progression of a tumor that is resistant to radiation (30–32). There is an urgent need to identify an adjunct therapy that, by enhancing the efficacy of radiation, can help lower the radiation dose and preserve hearing. In this study, we found the HGF/cMET signaling pathway to be activated in schwannomas resistant to RT. cMET is a major resistance mechanism to chemotherapy, RT, and targeted therapies: HGF expression and its subsequent cMET activation, via PI3K and Akt signaling pathways, protect cells from DNA fragmentation and apoptosis induced by chemotherapy and RT (16–18, 33–36). These studies suggest that combined treatment with cMET inhibitors may enhance radiosensitivity and circumvent the onset of resistance. Indeed, in our schwannoma models, we found that both pharmacological and

Table 1. Demographics and clinical characteristics of NF2 and sporadic VSs

Characteristic	No.	
	NF2 (n = 17)	Sporadic (n = 10)
Age, y		
Median	25	34
Range	8–52	26–42
Sex, %		
Male	10 (58.8)	5 (50.0)
Female	7 (41.2)	5 (50.0)
Tumor localization, %		
Left ear	8 (47.1)	4 (40.0)
Right ear	9 (52.9)	6 (60.0)
Tumor volume, mm^3		
Average	57,802	27,639
Range	5,400–125,000	960–52,500
Cyst formation, %	11 (64.7)	8 (80.0)
Brainstem compression, %	13 (76.5)	7 (70.0)
Tumor growing time, mo		
Average	65.7	27
Range	4–240	6–60

genetic blockade of cMET increased RT-induced DNA damage, and thus sensitized schwannomas to RT and lowered the RT dose needed to control tumor growth.

Previously, we showed that anti-VEGF treatment, via normalizing the tumor vasculature, increases tumor oxygen. Oxygen is a potent radiosensitizer; thus, combined anti-VEGF treatment enhances radiation efficacy (37). cMET activation can directly induce tumor angiogenesis by promoting endothelial cell proliferation, migration, and survival (38). Recent studies in VS cells also reported cross-talk between HGF/cMET and VEGF pathways: cMET targeting decreases VEGF and VEGF receptor 2 expression, while VEGF inhibition reduces cMET expression (21, 39, 40). However, in our animal studies, cMET blockade did not change VEGF expression; consequently, cMET blockade did not affect vessel density, perfusion, or tumor oxygenation. We found that cMET blockade enhances radiation sensitivity through a different mechanism, by enhancing radiation-induced tumor cell DNA damage. Which one of these adjunct strategies is more powerful in enhancing radiation efficacy, and whether their effects continue, saturate, or reverse, remains to be determined. In addition, our study points to a potential strategy of combined blockade of VEGF and cMET signaling with RT in treating schwannomas.

The mechanisms underlying deafness in NF2 are still unclear. One of the major limitations in studying tumor-induced hearing loss in mouse models of NF2 is the small size of the vestibular nerves, with their encasement in the bony internal auditory canal and the small size of the CPA angle posing significant technical challenges for orthotopic tumor implantation. VSs are intracranial, extraaxial tumors that arise from the Schwann cell sheath of the eighth cranial nerve. A recent study reported an allograft model of implanting schwannoma cells to the auditory–vestibular nerve complex, and tumor growth impaired hearing (41). However, because the tumor cells were injected through the internal auditory canal, the surgery and injection caused hearing loss that took up to 14 d to recover. In our novel CPA model, we implanted schwannoma cells directly into the CPA area, at the root entry zone of the eighth cranial nerve. We have shown in our model that (*i*) the surgery and injection do not directly affect hearing, (*ii*) tumor growth affects hearing, and (*iii*) the degree of hearing loss does not correlate with tumor size, indicating that our model faithfully represents the clinical findings in patients with VSs that tumor size and/or growth rate does not correlate with hearing loss (30, 42–45).

In several inner ear disorders, HGF/cMET signaling has been shown to protect cochlear hair cells from various types of damage, such as noise and oxidative stress induced by neomycin (25, 26). Local application of recombinant HGF attenuates noise-induced hearing loss in guinea pigs (27), and HGF gene transfer has been patented for the treatment of sensorineural hearing loss (26). These studies suggest that HGF has a therapeutic potential for hearing. However, a very interesting study reported two mouse models of *Hgf* dysregulation: (*i*) *Hgf* transgenic mice and (*ii*) mice with conditional knockout of the *Hgf* gene in the cochlea. In this study, overexpression of *Hgf* was associated with progressive degeneration of outer hair cells in the cochlea, and cochlear deletion of *Hgf* was also associated with dysplasia. This study concluded that both up- and down-regulation of HGF resulted in deafness (28). This raises the question of what the critical normal range of HGF is for individuals to have normal hearing. One study reported that in healthy adults (>18 y of age), plasma HGF levels are in the range of 196.6–477.9 pg/mL (46). In patients with NF2, Blakeley et al. (6) reported that plasma HGF levels are substantially higher (602.0–1,054 pg/mL). More importantly, they showed that the hearing response after anti-VEGF therapy inversely correlated with baseline HGF levels (6). These data suggest that HGF/cMET signaling may be involved in hearing loss and the hearing response after treatment in NF2 patients. CRZ is a cMET inhibitor; we found that it blocked cMET signaling in both NF2 tumors and stromal cells, and led to tumor control and radiosensitization. However, during the 3-wk treatment, CRZ did not improve hearing. This is potentially because CRZ treatment did not change HGF levels. This hypothesis cannot yet be tested directly as there are currently no anti-mouse HGF antibodies or inhibitors. Further biomarker studies for plasma HGF are needed to fully characterize the hearing response in future clinical studies of cMET blockade in

Table 2. Demographics and clinical characteristics of patients with NF2

Characteristic	No.
	Total (n = 29)
Age, y	
Median	31.7
Range	16–59
Sex, %	
Male	16 (55.2)
Female	13 (44.8)
Inheritance (sporadic), %	26 (89.7)
Previous radiotherapy, %	2 (6.9)
Tumor localization, %	
Left ear	11 (37.9)
Right ear	18 (62.1)
Tumor volume in target ear, mm^3	
Average	35,284.8
Range	720–90,896
Cyst formation, %	17 (58.6)
Brainstem compression, %	16 (55.2)
Tumor growing time, mo	
Average	61.8
Range	4–180
AAO-HNS hearing classification, %	
Class B	2 (6.9)
Class C	7 (24.1)
Class D	20 (69.0)

AAO-HNS, American Academy of Otolaryngology-Head and Neck Surgery Committee on Hearing and Equilibrium.

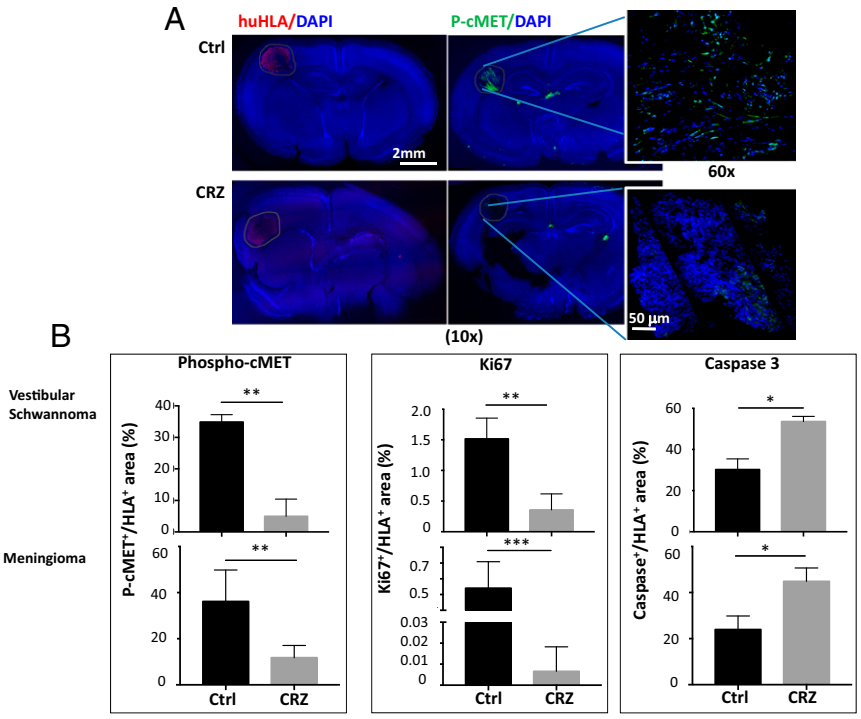

Fig. 6. cMET blockade inhibits the growth of patient-derived schwannomas in the organotypic brain slice culture model. (*A*) Representative immunofluorescently stained images of human NF2-deficient VSs (n = 3) and meningiomas (n = 4) [identified by human HLA (huHLA)$^+$; red] grown in the organotypic mouse brain slices (DAPI, blue) and their cMET phosphorylation level (P-cMET; green). Ctrl, control. (Magnification: 10×; *Insets*, 60×.) (*B*) Quantification of the fluorescent intensity of P-cMET, Ki67 (for tumor cell proliferation), and cleaved caspase-3 (for apoptosis). *$P < 0.05$; **$P < 0.01$; ***$P < 0.005$ (Student t test).

patients with schwannomas. Furthermore, we found that during the time period that CRZ achieves tumor growth control and radiosensitization, it did not cause significant damage to hearing in normal ears, suggesting that its use as an agent to control tumor growth is safe. We found a nonsignificant trend for elevated DPOAE thresholds after CRZ treatment, suggesting a potential toxic effect on outer hair cell function. Whether prolonged use of CRZ would eventually result in ABR changes or significantly worsening DPOAE thresholds would require experiments to fully characterize its long-term safety and potential toxicity.

Secreted factors, such as inflammatory cytokines, have been shown to cause cochlea damage and hearing loss via immune-mediated mechanisms (47, 48). Activation of the cMET pathway has been shown to mobilize an inflammatory network in the brain microenvironment to promote cancer progression (49, 50). In our studies, we observed that cMET blockade reduced Stat3 inflammatory signaling, but did not affect the infiltration of macrophages or the production of inflammatory cytokines (IL-1β, IFN-γ, IL-2, IL-6, and TNF-α). Part of the reason why we did not observe inflammatory changes could be because our study is limited to the use of immune-deficient nude mice to grow our xenograft tumors. Therefore, further studies in immune-competent, genetically engineered *Nf2* gene knockout mouse models are needed to fully characterize the contribution of the immune compartment to schwannoma-induced hearing loss and response to cMET blockade.

To evaluate the translational potential of cMET blockade in schwannomas, we first evaluated the expression/activation level of the target. HGF and cMET have been detected in schwannomas (19, 20), but no clear relationship between HGF/cMET expression and schwannoma progression has been reported. We report here that HGF expression correlates with cyst formation and, together with cMET activation, is an independent predictor of tumor volume, confirming HGF and cMET as valid targets in patients with NF2. Moreover, we tested CRZ treatment on patient-derived schwannomas. We grew the human schwannomas in the brain slices obtained from immune-deficient nude mice. It has been well documented that the tumor microenvironment affects tumor growth and its response to therapy (51, 52); the brain slices contain all of the brain host cell types and maintain the appropriate tumor–host contacts, and thus provide more accurate information on tumor response to therapy (53). Another advantage of organotypic brain slice culture is that it allows a longer period of time to monitor tumor response to treatment, up to 3 wk before the brain slices disintegrate. In contrast, the routine MTT assay only allows monitoring of tumor cell viability changes after treatment for several days before the cells become confluent in the well (96-well plate); therefore, the organotypic brain slice model more accurately reflected schwannoma growth and response to CRZ treatment.

In summary, our study demonstrated that integrating cMET blockade with RT in schwannoma models is more effective than either therapy alone. Our study provides the rationale and critical data for the clinical translation of combining cMET blockade with RT in patients with VSs.

Methods

Animal Models. We used two xenograft models in our study.

Sciatic nerve model. To reproduce the microenvironment of peripheral schwannomas, we implanted tumor cells into the mouse sciatic nerve (37). Three microliters of tumor cell suspension was injected slowly (over 45–60 s) under the sciatic nerve sheath using a Hamilton syringe to prevent leakage. Mice were killed when the tumor reached 1 cm in diameter.

CPA model. To recapitulate the intracranial microenvironment of VSs, we implanted transparent cranial windows into 8- to 10-wk-old nude mice as previously described (37). After 7–10 d, tumor cells were injected into the CPA region of the right hemisphere. In both models, 1×10^6 HEI193 cells and 1×10^5 NF2$^{-/-}$ cells were implanted per mouse.

Treatment Protocols. All animal procedures were performed following the guidelines of the Public Health Service Policy on Humane Care of Laboratory Animals and were approved by the Institutional Animal Care and Use Committee of the Massachusetts General Hospital and Massachusetts Eye and Ear.

CRZ treatment. Fifty milligrams per kilogram of PF-2341066 dispersed in water was administered by oral gavage each day, and was continued until mice in the control group became moribund.

RT. We irradiated schwannomas in a ^{137}Cs gamma-irradiator for small animals that produces 1.176-MeV gamma rays and allows longitudinal radiation studies. Mice were irradiated locally in our custom-designed irradiation chamber, which shields the entire animal except for the brain (in the CPA model) or the leg (in the sciatic nerve model) (37). We chose to use 5 Gy in

our study as it produced tumor growth delay with the least amount of toxicity (evaluated by body weight loss) (37).

Ethics Approval. Archived clinical VS tumor tissues and data were used in accordance with protocol approved by the Research Ethics Board at Beijing Tian Tan Hospital, China. Excess tissue used for organotypic culture was obtained following approval by the Partners Human Research Committee/IRB at Massachusetts General Hospital.

ACKNOWLEDGMENTS. We thank Shan Min Chin, Anna Khachatryan, and Carolyn Smith for their superb technical support; Sylvie Roberge and Dr. Peigen Huang for assistance in animal studies, tumor implantation, and cranial window generation; and Meenal Datta for editorial help with the manuscript. This study was supported by Department of Defense New Investigator Award W81XWH-16-1-0219 (to L.X.); American Cancer Society Research Scholar Award RSG-12-199-01-TBG (to L.X.); the Children's Tumor Foundation Drug Discovery Initiative (L.X.); the Ira Spiro Award (to L.X.); National Natural Science Foundation of China Grant 81372715 (to P.L.); Grants P01-CA080124, P50-CA165962, R01-CA129371, R01-CA208205, and U01-CA 224348 (to R.K.J.); National Cancer Institute Outstanding Investigator Award R35-CA197743 (to R.K.J.); the Lustgarten Foundation (R.K.J.); the Ludwig Center at Harvard (R.K.J.); the National Foundation for Cancer Research (R.K.J.); the Gates Foundation (R.K.J.); National Institute on Deafness and Other Communication Disorders Grant R01DC015824 (to K.M.S.); Department of Defense Grant W81XWH-14-1-0091 (to K.M.S.); the Bertarelli Foundation (K.M.S.); the Nancy Sayles Day Foundation (K.M.S.); the Lauer Tinnitus Research Center (K.M.S.); and National Natural Science Foundation of China Grant 81502657 (to Y.c.Z.).

1. Evans DG, et al. (1992) A clinical study of type 2 neurofibromatosis. *Q J Med* 84: 603–618.
2. Plotkin SR, Merker VL, Muzikansky A, Barker FG, 2nd, Slattery W, 3rd (2014) Natural history of vestibular schwannoma growth and hearing decline in newly diagnosed neurofibromatosis type 2 patients. *Otol Neurotol* 35:e50–e56.
3. Jimenez RB, et al. (2017) The impact of different stereotactic radiation therapy regimens for brain metastases on local control and toxicity. *Adv Radiat Oncol* 2:391–397.
4. Plotkin SR, et al. (2009) Hearing improvement after bevacizumab in patients with neurofibromatosis type 2. *N Engl J Med* 361:358–367.
5. Blakeley J, et al. (2014) Clinical response to bevacizumab in schwannomatosis. *Neurology* 83:1986–1987.
6. Blakeley JO, et al. (2016) Efficacy and biomarker study of bevacizumab for hearing loss resulting from neurofibromatosis type 2-associated vestibular schwannomas. *J Clin Oncol* 34:1669–1675.
7. Matsumoto K, Nakamura T (2006) Hepatocyte growth factor and the Met system as a mediator of tumor-stromal interactions. *Int J Cancer* 119:477–483.
8. Lesko E, Majka M (2008) The biological role of HGF-MET axis in tumor growth and development of metastasis. *Front Biosci* 13:1271–1280.
9. Steffan JJ, Coleman DT, Cardelli JA (2011) The HGF-met signaling axis: Emerging themes and targets of inhibition. *Curr Protein Pept Sci* 12:12–22.
10. Di Renzo MF, Poulsom R, Olivero M, Comoglio PM, Lemoine NR (1995) Expression of the Met/hepatocyte growth factor receptor in human pancreatic cancer. *Cancer Res* 55:1129–1138.
11. Scarpino S, et al. (1999) Hepatocyte growth factor (HGF) stimulates tumour invasiveness in papillary carcinoma of the thyroid. *J Pathol* 189:570–575.
12. Lubensky IA, et al. (1999) Hereditary and sporadic papillary renal carcinomas with c-met mutations share a distinct morphological phenotype. *Am J Pathol* 155:517–526.
13. Gentile A, Trusolino L, Comoglio PM (2008) The Met tyrosine kinase receptor in development and cancer. *Cancer Metastasis Rev* 27:85–94.
14. Gherardi E, Sharpe M, Lane K, Sirulnik A, Stoker M (1993) Hepatocyte growth factor/scatter factor (HGF/SF), the c-met receptor and the behaviour of epithelial cells. *Symp Soc Exp Biol* 47:163–181.
15. Weidner KM, et al. (1993) Molecular characteristics of HGF-SF and its role in cell motility and invasion. *EXS* 65:311–328.
16. Bhardwaj V, et al. (2013) Modulation of c-Met signaling and cellular sensitivity to radiation: Potential implications for therapy. *Cancer* 119:1768–1775.
17. Delitto D, Vertes-George E, Hughes SJ, Behrns KE, Trevino JG (2014) c-Met signaling in the development of tumorigenesis and chemoresistance: Potential applications in pancreatic cancer. *World J Gastroenterol* 20:8458–8470.
18. Garajová I, Giovannetti E, Biasco G, Peters GJ (2015) c-Met as a target for personalized therapy. *Transl Oncogenomics* 7:13–31.
19. Moriyama T, et al. (1998) Comparative analysis of expression of hepatocyte growth factor and its receptor, c-met, in gliomas, meningiomas and schwannomas in humans. *Cancer Lett* 124:149–155.
20. Torres-Martin M, et al. (2013) Microarray analysis of gene expression in vestibular schwannomas reveals SPP1/MET signaling pathway and androgen receptor deregulation. *Int J Oncol* 42:848–862.
21. Dilwali S, Roberts D, Stankovic KM (2015) Interplay between VEGF-A and cMET signaling in human vestibular schwannomas and schwann cells. *Cancer Biol Ther* 16: 170–175.
22. Krasnoselsky A, et al. (1994) Hepatocyte growth factor is a mitogen for Schwann cells and is present in neurofibromas. *J Neurosci* 14:7284–7290.
23. Troutman S, et al. (2016) Crizotinib inhibits NF2-associated schwannoma through inhibition of focal adhesion kinase 1. *Oncotarget* 7:54515–54525.
24. Nadol JB, Jr, Diamond PF, Thornton AR (1996) Correlation of hearing loss and radiologic dimensions of vestibular schwannomas (acoustic neuromas). *Am J Otol* 17: 312–316.
25. Kikkawa YS, et al. (2009) Hepatocyte growth factor protects auditory hair cells from aminoglycosides. *Laryngoscope* 119:2027–2031.
26. Oshima K, et al. (2004) Intrathecal injection of HVJ-E containing HGF gene to cerebrospinal fluid can prevent and ameliorate hearing impairment in rats. *FASEB J* 18: 212–214.
27. Inaoka T, et al. (2009) Local application of hepatocyte growth factor using gelatin hydrogels attenuates noise-induced hearing loss in Guinea pigs. *Acta Otolaryngol* 129:453–457.
28. Schultz JM, et al. (2009) Noncoding mutations of HGF are associated with nonsyndromic hearing loss, DFNB39. *Am J Hum Genet* 85:25–39.
29. Organ SL, Tsao MS (2011) An overview of the c-MET signaling pathway. *Ther Adv Med Oncol* 3(1 Suppl):S7–S19.
30. Masuda A, Fisher LM, Oppenheimer ML, Iqbal Z, Slattery WH; Natural History Consortium (2004) Hearing changes after diagnosis in neurofibromatosis type 2. *Otol Neurotol* 25:150–154.
31. Ammoun S, Hanemann CO (2011) Emerging therapeutic targets in schwannomas and other merlin-deficient tumors. *Nat Rev Neurol* 7:392–399.
32. Plotkin SR, et al. (2012) Bevacizumab for progressive vestibular schwannoma in neurofibromatosis type 2: A retrospective review of 31 patients. *Otol Neurotol* 33: 1046–1052.
33. Fan S, et al. (1998) Scatter factor protects epithelial and carcinoma cells against apoptosis induced by DNA-damaging agents. *Oncogene* 17:131–141.
34. Medová M, Aebersold DM, Zimmer Y (2012) MET inhibition in tumor cells by PHA665752 impairs homologous recombination repair of DNA double strand breaks. *Int J Cancer* 130:728–734.
35. Yuan R, et al. (2001) Altered gene expression pattern in cultured human breast cancer cells treated with hepatocyte growth factor/scatter factor in the setting of DNA damage. *Cancer Res* 61:8022–8031.
36. Hu SY, et al. (2009) Hepatocyte growth factor protects endothelial cells against gamma ray irradiation-induced damage. *Acta Pharmacol Sin* 30:1415–1420.
37. Gao X, et al. (2015) Anti-VEGF treatment improves neurological function and augments radiation response in NF2 schwannoma model. *Proc Natl Acad Sci USA* 112: 14676–14681.
38. Birchmeier C, Birchmeier W, Gherardi E, Vande Woude GF (2003) Met, metastasis, motility and more. *Nat Rev Mol Cell Biol* 4:915–925.
39. Zhang YW, Su Y, Volpert OV, Vande Woude GF (2003) Hepatocyte growth factor/scatter factor mediates angiogenesis through positive VEGF and negative thrombospondin 1 regulation. *Proc Natl Acad Sci USA* 100:12718–12723.
40. Sulpice E, et al. (2009) Cross-talk between the VEGF-A and HGF signalling pathways in endothelial cells. *Biol Cell* 101:525–539.
41. Bonne NX, et al. (2016) An allograft mouse model for the study of hearing loss secondary to vestibular schwannoma growth. *J Neurooncol* 129:47–56.
42. Asthagiri AR, et al. (2012) Mechanisms of hearing loss in neurofibromatosis type 2. *PLoS One* 7:e46132.
43. Abaza MM, Makariou E, Armstrong M, Lalwani AK (1996) Growth rate characteristics of acoustic neuromas associated with neurofibromatosis type 2. *Laryngoscope* 106: 694–699.
44. Fisher LM, Doherty JK, Lev MH, Slattery WH (2009) Concordance of bilateral vestibular schwannoma growth and hearing changes in neurofibromatosis 2: Neurofibromatosis 2 natural history consortium. *Otol Neurotol* 30:835–841.
45. Graamans K, Van Dijk JE, Janssen LW (2003) Hearing deterioration in patients with a non-growing vestibular schwannoma. *Acta Otolaryngol* 123:51–54.
46. Kleiner G, Marcuzzi A, Zanin V, Monasta L, Zauli G (2013) Cytokine levels in the serum of healthy subjects. *Mediators Inflamm* 2013:434010.
47. Dilwali S, Landegger LD, Soares VY, Deschler DG, Stankovic KM (2015) Secreted factors from human vestibular schwannomas can cause cochlear damage. *Sci Rep* 5: 18599.
48. Vambutas A, Pathak S (2016) AAO: Autoimmune and autoinflammatory (disease) in otology: What is new in immune-mediated hearing loss. *Laryngoscope Investig Otolaryngol* 1:110–115.
49. Xing F, et al. (2016) Activation of the c-Met pathway mobilizes an inflammatory network in the brain microenvironment to promote brain metastasis of breast cancer. *Cancer Res* 76:4970–4980.
50. Spina A, et al. (2015) HGF/c-MET axis in tumor microenvironment and metastasis formation. *Biomedicines* 3:71–88.
51. Langley RR, Fidler IJ (2011) The seed and soil hypothesis revisited–The role of tumor-stroma interactions in metastasis to different organs. *Int J Cancer* 128:2527–2535.
52. Jain RK (2013) Normalizing tumor microenvironment to treat cancer: Bench to bedside to biomarkers. *J Clin Oncol* 31:2205–2218.
53. Humpel C (2015) Organotypic brain slice cultures: A review. *Neuroscience* 305:86–98.